Glomerular sclerosis in kidneys with congenital nephrotic syndrome (NPHS1)

A-M Kuusniemi[1], J Merenmies[1], A-T Lahdenkari[1], C Holmberg[1], K Salmela[2], R Karikoski[1], J Rapola[1] and H Jalanko[1]

[1]Hospital for Children and Adolescents and Biomedicum Helsinki, University of Helsinki, Helsinki, Finland and [2]Kidney Transplantation Unit, Helsinki University Hospital, Helsinki, Finland

Congenital nephrotic syndrome of the Finnish type (NPHS1) is a rare genetic disease caused by mutations in the NPHS1 gene encoding a major podocyte slit-diaphragm protein, nephrin. Patients with NPHS1 have severe nephrotic syndrome from birth and develop renal fibrosis in early childhood. In this work, we studied the development of glomerular sclerosis in kidneys removed from 4- to 44-month-old NPHS1 patients. The pathological lesions and expression of glomerular cell markers were studied in nephrectomized NPHS1 and control kidneys using light and electron microscopy and immunohistochemistry. An analysis of 1528 glomeruli from 20 patients revealed progressive mesangial sclerosis and capillary obliteration. Although few inflammatory cells were detected in the mesangial area, paraglomerular inflammation and fibrosis was common. The podocytes showed severe ultrastructural changes and hypertrophy with the upregulation of cyclins A and D1. Podocyte proliferation, however, was rare. Apoptosis was hardly detected and the expression of antiapoptotic B-cell lymphoma-2 and proapoptotic p53 were comparable to controls. Moderate amounts of podocytes were secreted into the urine of NPHS1 patients. Shrinkage of the glomerular tuft was common, whereas occlusion of tubular opening or protrusion of the glomerular tuft into subepithelial space or through the Bowman's capsule were not detected. The results indicate that, in NPHS1 kidneys, the damaged podocytes induce progressive mesangial expansion and capillary obliteration. Podocyte depletion, glomerular tuft adhesion, and misdirected filtration, however, seem to play a minor role in the nephron destruction.

Constant proteinuria is known to result in glomerular sclerosis and tubulointerstitial fibrosis, often gradually leading to terminal renal failure.[1] Recent studies have indicated that injury in glomerular epithelial cells (podocytes) leads to proteinuria and also triggers progressive glomerular sclerosis. Mutations in genes encoding for podocyte proteins such as podocin, CD2-associated protein and α-actinin-4 result in proteinuria and the development of lesions classified as focal segmental glomerulosclerosis (FSGS).[2,3] Congenital nephrotic syndrome caused by mutations in WT1 gene, on the other hand, is associated with diffuse mesangial sclerosis.[4]

In this work, we analyzed the glomerular changes in kidneys with congenital nephrotic syndrome of the Finnish type (CNF, NPHS1), which is a recessively inherited renal disease caused by mutations in the nephrin gene.[5] Nephrin is a podocyte-specific protein located at the slit diaphragm of kidney glomerulus. Many of the NPHS1 mutations, such as Fin-major and Fin-minor, lead to the absence of nephrin and severe nephrotic syndrome starting from the birth.[6] The NPHS1 kidneys show disrupted slit diaphragms and effacement of podocyte foot processes seen in many other proteinuric kidney diseases.[6,7] Children with NPHS1 are nephrectomized as infants (usually under the age of 1 year) when the renal function is still well preserved. These kidneys serve as a unique human material to study the development of glomerulosclerosis. This is emphasized by the fact that the basic defect is restricted to podocytes; it affects equally all glomeruli and the scarring in NPHS1 kidneys progresses in a fast manner as compared to many other disorders.

During the past years, proteinuria has been associated with a number of morphologic variants of glomerular sclerosis, both in human diseases and animal models.[8,9] Also, a sequence of pathological events has been suggested, which starts with podocyte depletion and formation of glomerular tuft adhesions with Bowman's capsule resulting in misdirected filtration and destruction of the nephrons.[10–12] Based on these findings, we were especially interested in the lesions detectable in the endo- and extracapillary compartments of NPHS1 glomeruli in the early phase of the sclerotic process.

RESULTS

The overall histology of the 49 NPHS1 kidneys nephrectomized at the age of 4–44 months ranged from nearly normal to severely damaged (Figure 1). The findings included glomerular sclerosis, interstitial fibrosis and inflammation, tubular atrophy and dilatation, and arterial wall thickening. Variation in the rate of progression of the pathological lesions was evident, so that fairly normal and totally sclerotic glomeruli and tubuli could be seen next to each other (Figure 1a). Affected glomeruli were scattered around the whole cortex, without predilection to juxtamedullary area as often seen in FSGS. Clusters of inflammatory cells were common around degenerating glomeruli in NPHS1 kidneys (Figures 1b, 2e, and 3j).

Mesangial expansion and capillary obliteration were early and constant findings

Histopathology of 1528 glomeruli in 20 NPHS1 kidneys from patients with different ages was systematically analyzed (Figure 2). Mesangium was affected in practically every glomerulus (99.7%), so that the lesions ranged from mild widening of the mesangial stalk to total sclerosis (Figure 3a–e). The early lesions were scattered around the glomerular tuft and consisted of increased number of mesangial cells and matrix (Figure 3b). The number of proliferating cells, as revealed by the MIB-1 staining, was increased in the NPHS1 (1.14 ± 0.44/glomerular gross section) as compared to controls (0.2 ± 0.14/GCS) ($P < 0.0005$). On the other hand, few terminal deoxynucleotidyl transferase-mediated dUTP

nick-end labeling (TUNEL)-positive apoptotic cells were present in the glomerular tuft both in NPHS1 kidneys and controls (0.01 ± 0.01/GCS and 0.07 ± 0.07/GCS, respectively).
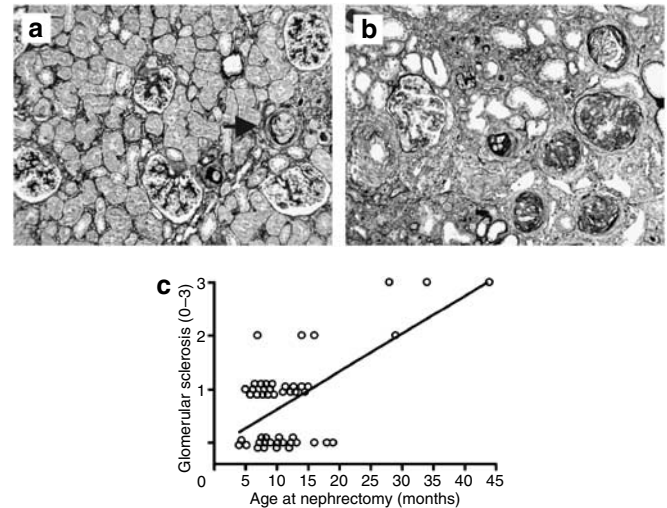

Figure 1 | Progression of renal damage in NPHS1 kidneys.
(**a**) A typical finding in a fairly well-preserved NPHS1 kidney (nephrectomized at the age of 7 months): one totally sclerosed glomerulus (arrow) surrounded by several glomeruli with only mild mesangial expansion. (**b**) Severe glomerular sclerosis, arterial wall thickening, and tubulointerstitial damage in an NPHS1 kidney removed at the age of 29 months. (**c**) Development of glomerular sclerosis (scored 0–3) in 49 NPHS1 kidneys in relation to the patients age at the time of nephrectomy. The rate of progression of glomerular sclerosis varies considerably among the patients ($r^2 = 0.40$). (**a** and **b**; PASM stainings, original magnification × 50).
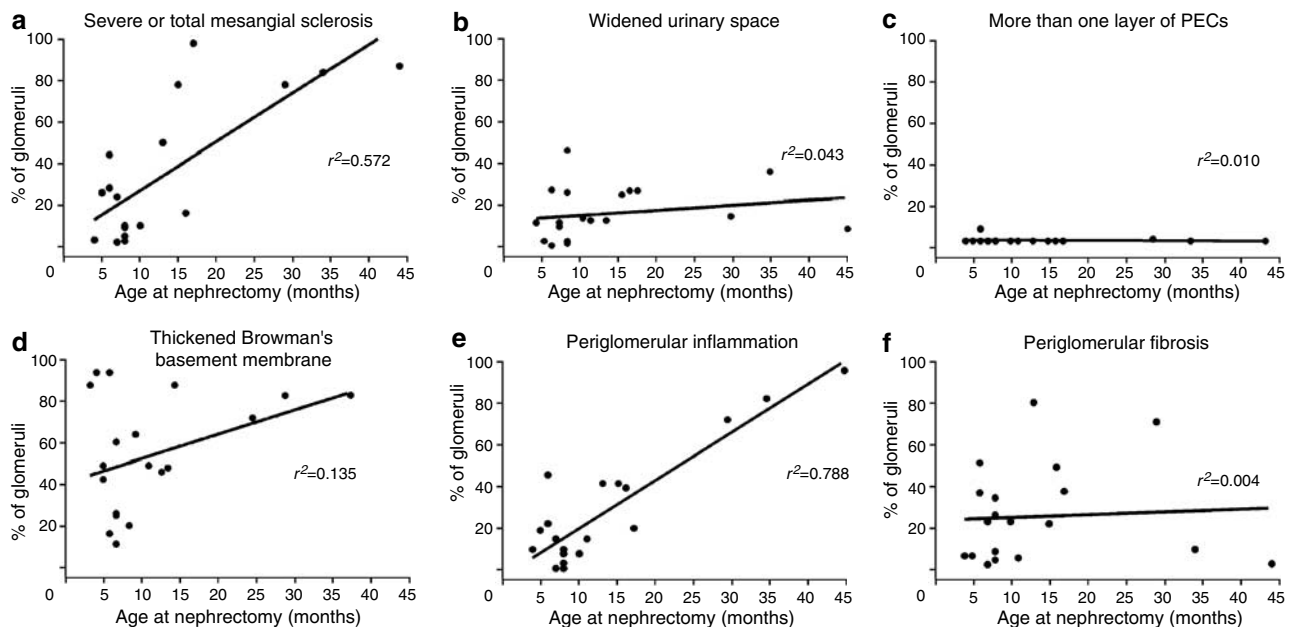

Figure 2 | Glomerular histology in relation to the age of the patients at the time of nephrectomy. The results are based on a semiquantitative analysis of glomerular histology (see Materials and Methods for more details). One thousand five hundred and twenty-eight glomeruli from PASM-stained samples in kidneys of 20 patients (age 4–44 months) with NPHS1 were analyzed. (**a**) The proportion of glomeruli with extensive mesangial sclerosis was higher in older kidneys. (**b**) The prevalence of wide urinary space was around 20% in all NPHS1 samples. (**c**) A single-cell layer of PECs was found in over 99% of NPHS1 glomeruli. (**d**) There was great variation in the rate of Bowman's capsule thickening between the samples. (**e**) Development of periglomerular inflammatory cell infiltration had the strongest correlation with age ($r^2 = 0.79$). (**f**) Periglomerular fibrosis surrounding the glomerulus did not correlate with age.
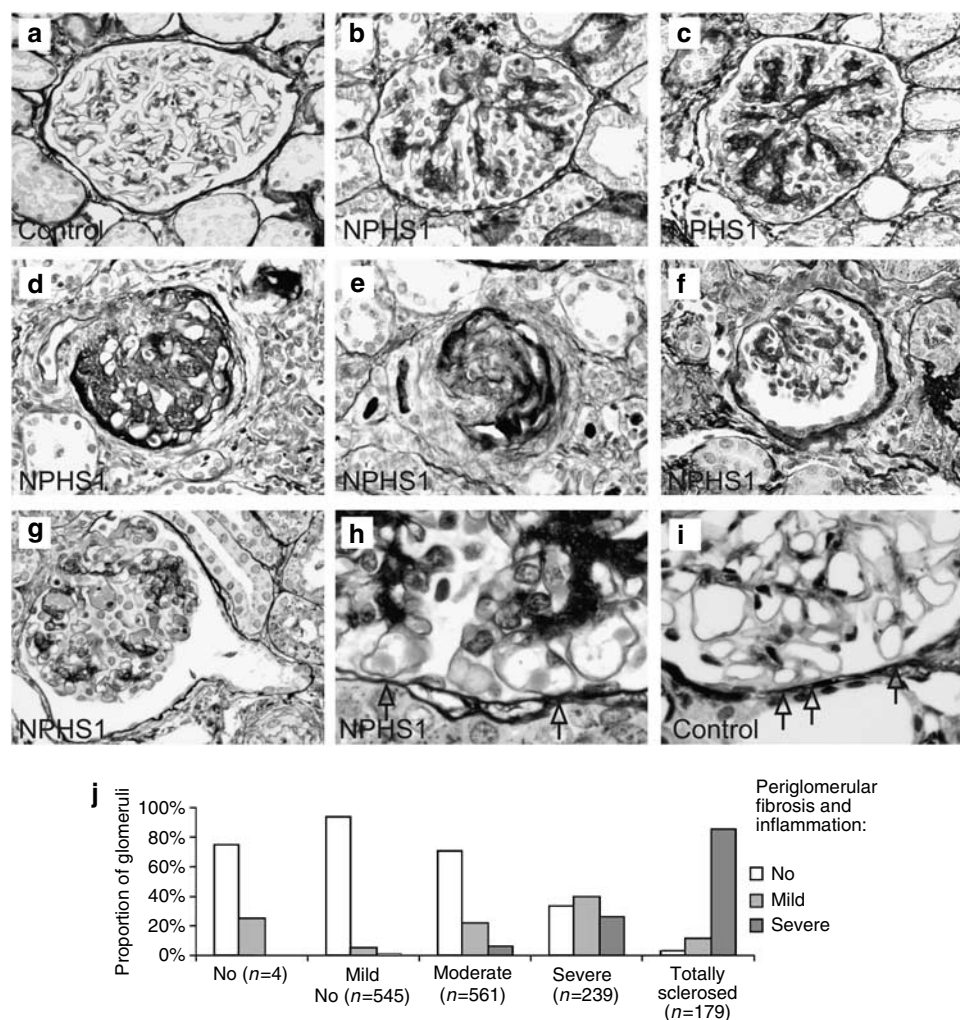
Figure 3 | Light microscopic findings in NPHS1 kidneys. (**a**) Control kidney glomerulus with normal mesangium. (**b–e**) A series of NPHS1 glomeruli with increasing amount of mesangial sclerosis. Some degree of mesangial sclerosis was found in 99.7% of NPHS1 glomeruli. (**f**) Urinary space (Bowman space) was wide in 18% of NPHS1 glomeruli analyzed. Hypertrophic single-cell layer was observed in 9% of the glomeruli, and in 87% of these glomeruli, the Bowman's basement membrane was thickened. (**g**) There were very few tip lesions and no peritubular changes in NPHS1 glomeruli. (**h** and **i**) High-magnification images showing a common finding in NPHS1 and control kidneys: glomerular tuft seems to be in contact with the Bowman's capsule (arrows). (**j**) Correlation of the mesangial sclerosis with periglomerular fibrosis and inflammation. (**a–i**; PASM stainings, original magnification $\times 200$ in (**a**)–(**g**) and $\times 500$ in (**h**) and (**i**)).

Inflammatory cells were rare in the capillary tuft as studied by immunohistochemistry, with a mean of 3.7 ± 1.8 and 1.1 ± 0.2 cells/GCS in NPHS1 and control kidneys, respectively ($P < 0.05$). The cells were mainly lymphocytes with cells of the monocyte/macrophage lineage (expressing CD14, CD13, and CD68 markers) as the second largest group (Figure 4).

Obliteration of glomerular capillaries could be seen already in glomeruli with mild and moderate mesangial changes (Figure 5). Immunoperoxidase staining for the endothelial marker CD34 clearly demonstrated a decrease in the total endothelial surface area of the capillary tuft ($P < 0.05$) (Figure 5e) and narrowing of the capillary lumens in NPHS1 kidneys as compared to controls ($P < 0.005$) (Figure 5f). Endothelial cell swelling was evident in direct microscopy (Figure 6c and d), but capillary thrombosis or

hyaline occlusion was not seen among 230 NPHS1 glomeruli from 11 patients studied with light microscopy of HE staining. Collapse of the capillary tuft was evident in glomeruli with severe mesangial lesions.

Podocytes showed phenotypic changes and hypertrophy, but little proliferation or apoptosis

Podocytes in NPHS1 kidney show marked structural changes as shown previously.[7] Prominent podocyte cell bodies with microvillous degeneration, elongated primary processes, and foot process effacement was most evident in scanning electron microscopy (Figure 6a and b). Also in light microscopy, podocytes in NPHS1 kidneys looked hypertrophic with prominent nucleus (Figure 6c and d).

The number of WT1-positive cells (podocytes) in well-preserved NPHS1 glomeruli was similar to controls
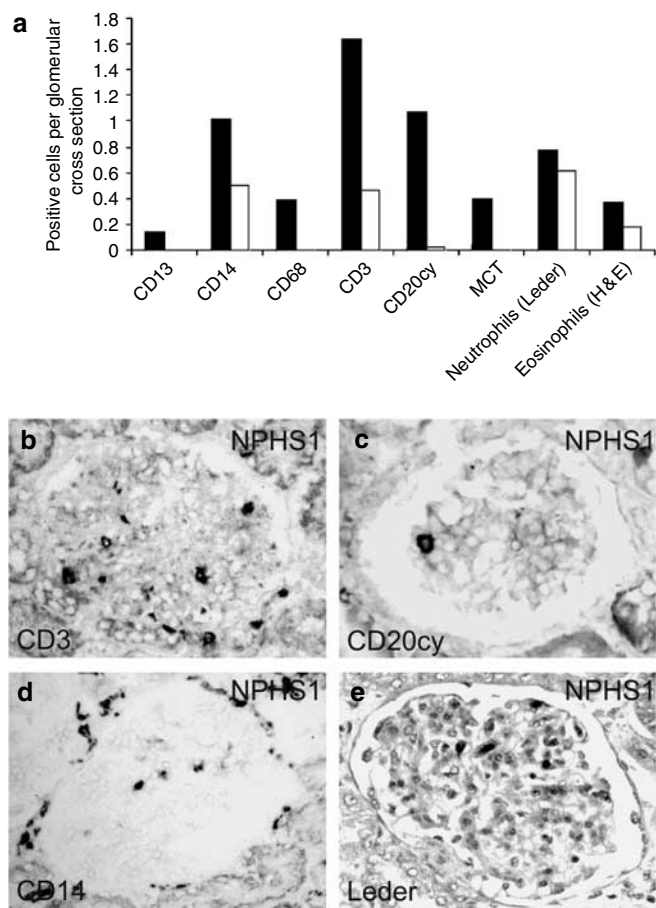
Figure 4 | Light microscopy and immunoperoxidase staining of inflammatory cells in NPHS1 and control glomeruli. There was an average of 3.7 and 1.1 inflammatory cells per glomerular cross-section in NPHS1 and control kidneys, respectively. (**a**) The numbers of different inflammatory cell types in NPHS1 (■) and control (□) glomeruli. (**b**) CD3-positive T-lymphocytes were the largest group, followed by (**c**) CD20-positive B-lymphocytes. The cells of monocyte/macrophage lineage including (**d**) CD14-positive cells were the second largest group after lymphocytes. Smaller amounts of (**e**) neutrophils, mast cells (mast cell Tryptase), and eosinophils were present. Original magnification × 200.

Figure 5 | Capillary changes in NPHS1 glomeruli. (**a–d**) Immunoperoxidase staining of endothelial cell marker CD34 showing narrowing of the capillary lumen in NPHS1 kidneys as compared to controls. (**e**) The area fraction of CD34 demonstrating the amount of endothelium present in a glomerulus was significantly lower in NPHS1 than in control glomeruli. (**f**) Also, the area fraction of areas inside the CD34-stained capillary walls was significantly lower in NPHS1 glomeruli. The area fractions were calculated from a total of 210 glomeruli. Original magnification × 200.

$(33.2 \pm 5.5$ and $36.3 \pm 2.8/GCS$, respectively) (Figure 7a–c). The area fraction of the podocyte intermediate filament, vimentin, was slightly reduced in NPHS1 glomeruli with mild lesions as compared to controls (Figure 7d–f). In clearly sclerotic glomeruli, the expression of both markers was decreased indicating podocyte loss (Figure 7c and f).

The number of MIB-1-positive proliferating extracapillary cells was low (0.08/GCS) in NPHS1 kidneys (Table 1, Figure 8a). Also, podocyte layer hyperplasia, as seen in collapsing glomerulopathy, was suspected in only 11 of 1528 (1%) NPHS1 glomerular cross-sections, all of them showing severe mesangial lesions.

Even though podocyte proliferation was nearly absent, there was upregulation of cell cycle promoters cyclin A and especially cyclin D1 and downregulation of cell cycle kinase inhibitor p57 in NPHS1 compared to controls (Table 1, Figure 8c–h). Thi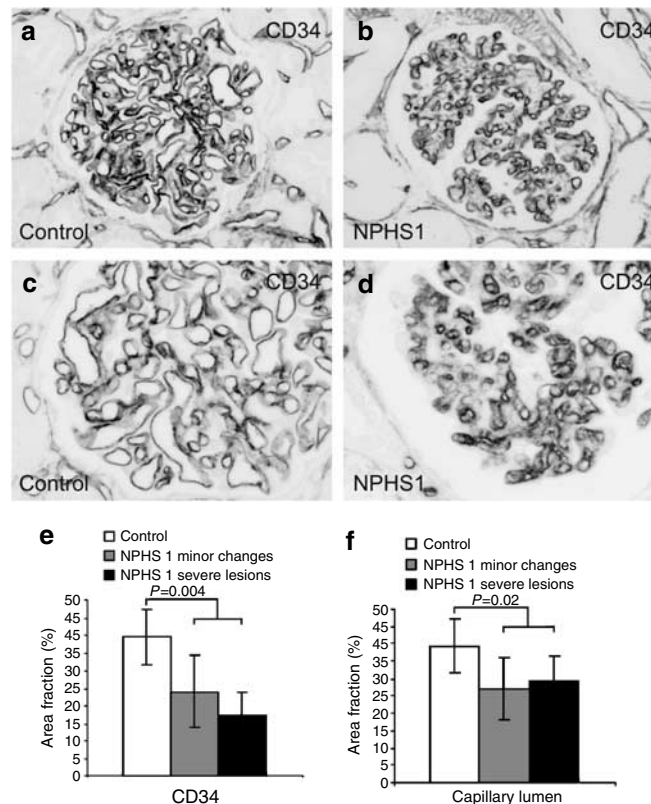s indicates that podocytes were in a hypertrophic state, which was also supported by the findings in light microscopy (see above).

Apoptosis of podocytes was not prominent, as no TUNEL-positive extracapillary cells were found in NPHS1 glomeruli (Table 1, Figure 8b). In accordance with this, no extracapillary cells with condensed nuclei (apoptosis or mitosis) were detected in NPHS1 glomeruli (Table 1). Although the expression of proapoptotic p53 was not increased in the extracapillary cells (Table 1, Figure 8i and j), the number of cells expressing the antiapoptotic B-cell lymphoma-2 was slightly but not significantly higher in NPHS1 glomeruli (0.05/GCS) than in controls (0.01/GCS) ($P = NS$) (Table 1, Figure 8k and l).

Possible detachment of podocytes was evaluated by counting WT1-positive cells in tubular lumens of formalin-fixed tissue samples. There were no WT1-positive cells in 2130 NPHS1 and 1280 control tubular cross-sections. Excretion of podocytes into voided urine was analyzed using immunofluorescence staining of podocalyxin and ZO-1-positive cells and granules in 18 (of which 15 were used in immunohistology double stainings) urine samples from NPHS1 patients (age range 3–10 months) and 12 control

samples. Urine from NPHS1 patients contained more podocalyxin-positive cells (median 15.9 vs 0.7 cells/ml) and granules (total scores: 24.9 vs 1.5) than control urine samples (Figure 9a, c, and e). Double immunostaining for podocalyxin and ZO-1 revealed a median of 13.9 and 0.3 copositive cells in NPHS1 and control urine samples, respectively (Figure 9b, d, and f).
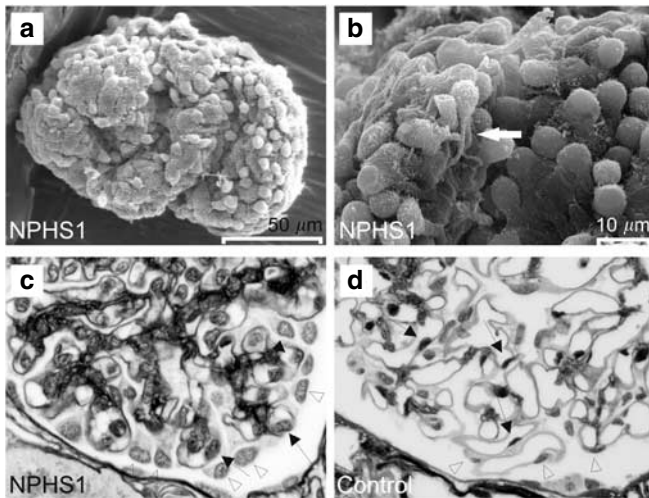

Figure 6 | Podocytes in NPHS1 glomeruli. (**a**, **b**) Scanning electron microscopy of NPHS1 glomeruli showing prominent cell bodies, abundant microvillar structures, long primary processes (white arrow), and foot process effacement. (**c**) Light microscopy of NPHS1 kidneys showing podocytes with large, hypertrophied cell bodies and larger nuclei that were located far from the basement membrane (arrowheads). Endothelial cells were also hypertrophic in NPHS1 glomeruli (arrows). (**d**) Normal podocytes (arrowheads) and endothelial cells (arrows) in a control kidney. (**c** and **d**; PASM stainings, original magnification × 500).

Parietal epithelial cells were resistant to protein overload

Parietal epithelial cell (PEC) layer looked normal in 91% (1097/1205) of the glomeruli that were included in the analysis. Hypertrophic single-cell layer was observed in 9% of the glomeruli, mostly (87%) in association with thickened basement membrane (Figure 3f). Only one glomerulus with more than one PEC layer was observed. Eighteen and five PECs with condensed nucleus (apoptosis/mitosis) per 100 glomeruli were observed in NPHS1 and controls, respectively ($P < 0.05$). PECs positive for the proliferation marker MIB-1 were somewhat more frequent in NPHS1 kidneys than controls (18 vs 3 per 100 glomeruli, $P = $ NS). On the other hand, only one TUNEL-positive apoptotic PEC was found in 836 NPHS1 glomeruli. The results indicate that PECs were quite resistant to the unusually high protein concentration of the primary filtrate.

No protrusion of the capillary tuft into peritubular or periglomerular spaces was observed

Urinary space (Bowman space) was wide in 18% (221/1227) of the NPHS1 glomeruli (Figure 2b). Two-thirds of these showed at least moderate sclerosis, suggesting that the widening was caused by shrinkage of the glomerular tuft. This was supported by the fact that the average area of glomeruli with normal ($n = 204$) and wide urinary space ($n = 103$) was quite similar (11835 ± 1972 vs 13516 ± 3021 pixels; $P = $ NS), respectively.

Contact of the capillary tuft with the Bowman's capsule was quite common both in NPHS1 and control kidneys (Figure 3h and i). Protrusion of the capillary tuft through Bowman's capsule, however, was not seen in any of the 1415 glomeruli specifically analyzed. Adhesion of the capillary tuft and Bowman's capsule at the tubular opening (tip lesion) was suspected in only four of the 207 (2%) glomeruli in which tubular opening was visible (Figure 3g). Similarly, separation
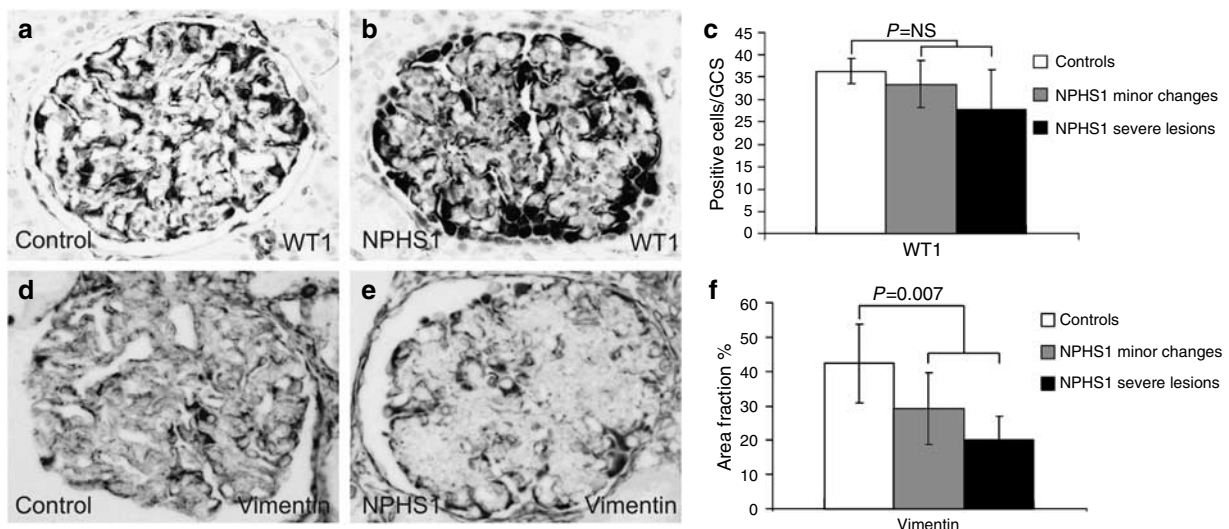

Figure 7 | The expression of WT1 and vimentin in NPHS1 and control kidneys. (**a–c**) The number of WT1-positive cells per glomerular cross-section in NPHS1 and control kidneys. (**d–f**) Area fraction of vimentin staining in NPHS1 kidneys. Original magnification × 200.

Table 1 | Expression of markers for cell cycle and apoptosis in NPHS1 and control glomeruli[a]

	NPHS1	Control	P-value
MIB-1	0.08 ± 0.07 (25/354)	0.03 ± 0.02 (5/180)	NS
TUNEL	0 (0/658)	~ 0 (1/240)	NS
Condensed nucleus	0 (0/635)	~ 0 (2/414)	NS
p57[b]	17.83 ± 2.75 (2852/160)	24.38 ± 3.51 (2438/100)	0.003
Cyclin A	0.03 ± 0.03 (20/582)	0 (0/310)	0.04
Cyclin D1	0.51 ± 0.32 (157/337)	0.10 ± 0.16 (18/224)	0.03
p53	0.06 ± 0.08 (19/351)	0.01 ± 0.01 (1/164)	NS
Bcl-2	0.05 ± 0.04 (20/378)	0.01 ± 0.01 (3/281)	NS

Abbreviations: Bcl, B-cell lymphoma; MIB, mind bomb homolog; NPHS1, nephrotic syndrome of the Finnish type; NS, nonsignificant; TUNEL, terminal deoxynucleotidyl transferase-mediated dUTP nick-end labeling.
[a]Results are expressed as the mean $\pm$ s.d. of positive cells per glomerular cross-section. In parenthesis: positive cells/glomerular cross-sections examined. Positive extracapillary cells counted only (except in the case of p57).
[b]All p57-positive glomerular cells counted, as p57 is expressed only in podocytes.
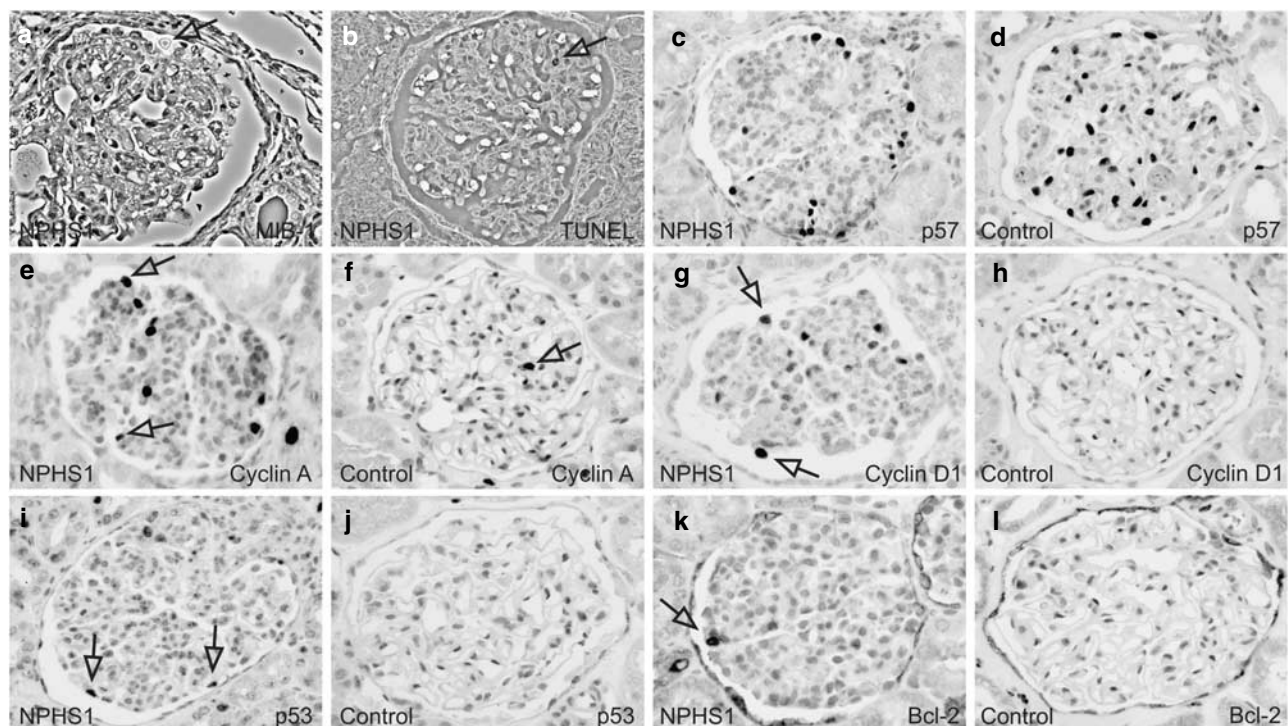

Figure 8 | Cell cycle markers of extracapillary cells in NPHS1 and control glomeruli. (**a**) There were very few (0.08/GCS) proliferating extracapillary cells (arrow) in NPHS1 kidneys based on the expression of MIB-1. (**b**) Apoptosis was even more uncommon among extracapillary cells in NPHS1. Few (0.01/GCS) TUNEL-positive cells (arrow) were however found within the tufts. (**c**) There were significantly less p57-positive cells in NPHS1 than in (**d**) control glomeruli. (**e–h**) On the other hand, there were more cyclin A- and cyclin D1-positive extracapillary cells in NPHS1 glomeruli than in controls ($P < 0.05$). (**i–l**) On average, one p53- and one B-cell lymphoma-2-positive extracapillary cell was found among 20 GCS. Although they were more frequent in NPHS1, the difference to controls was not statistically significant. (**a** and **c–l**; immunohistochemical stainings). Original magnification $\times 200$.

of tubular basement membrane from its epithelium and formation of a peritubular space was not seen among the tubular openings observed. Segmental crescent was seen in only 0.5% (5/1156) of the glomeruli analyzed.

DISCUSSION

We evaluated the development glomerular lesions in NPHS1 kidneys lacking the major podocyte slit-diaphragm protein nephrin. The analysis indicated that constant heavy proteinuria in these kidneys inevitably resulted in total glomerular sclerosis and destruction of the nephrons. The progression rate varied from nephron to nephron, suggesting that protein leakage, affecting equally all glomeruli, was not the only contributing factor for sclerosis. Impact of the damaged podocytes on the mesangial and endothelial cells was most probably crucial for the pathological process.

The most constant glomerular finding was mesangial sclerosis as reported previously.[13,14] Accumulation of extracellular matrix proteins and cells in the mesangium was evident in practically every glomerulus. Immunohistochemistry
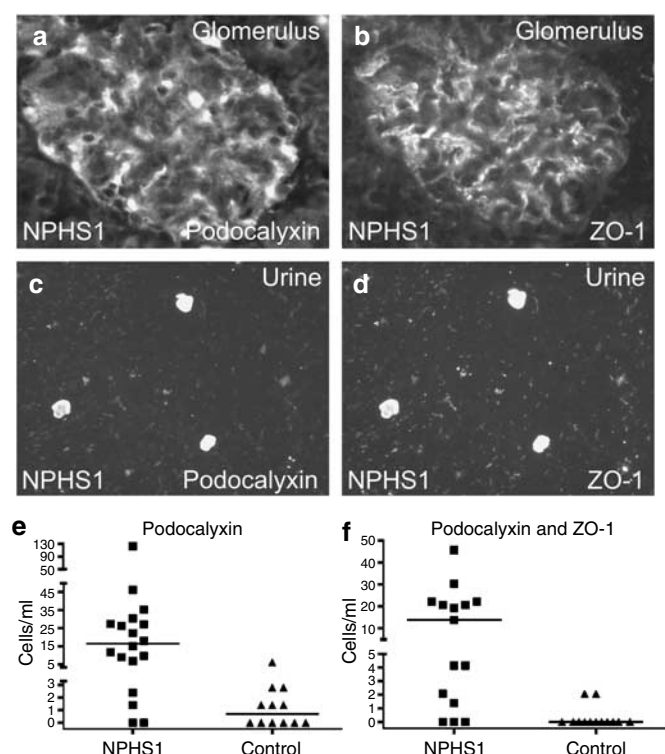
Figure 9 | Immunofluorescence staining of podocytes in the urine of NPHS1 patients and controls. (**a**) Immunofluorescence for podocalyxin in NPHS1 kidneys. Podocalyxin is found in podocytes and endothelial cells. (**b**) ZO-1 is specific for podocytes in the glomerulus. (**c**) Podocalyxin- and (**d**) ZO-1-positive cells in NPHS1 urine (images from immunofluorescence double staining). (**e**) Urine from NPHS1 patients contained more podocalyxin-positive cells (median 15.9 vs 0.7 cells/ml) than control urine samples. (**f**) Double immunostaining for podocalyxin and ZO-1 revealed a median of 13.9 and 0.3 co-positive cells in NPHS1 and control urine samples, respectively. The line indicates the median (in **e** and **f**). Original magnification $\times$ 200.

revealed that the glomerular tuft contained low numbers of inflammatory cells, indicating that the increased cellularity was caused by reactive mesangial cells. Especially the low number of monocytes/macrophages was interesting, as these cells have been suggested to play a central role in crescent formation and glomerulosclerosis.[15,16] The early lesions in the glomerular tuft did not show predilection to perihilar or urinary pole, as is the case in some types of FSGS.[17,18] Also, tip lesions, that would occlude the opening of the tubular lumen, were practically non-existing in NPHS1 kidneys.

Mesangial lesions were associated with obliteration of the glomerular capillaries. This was observed in the direct microscopy and immunohistochemical staining and was evident already in glomeruli with mild lesions. Also, the thickening of arteriolar walls in NPHS1 kidneys is a constant finding[19] and further highlights the important role of defective blood circulation in the scarring process.[20,21]

Based on morphological analyses of FSGS kidneys, Kriz and others.[10–12] have developed a widely accepted theory that, in proteinuric kidneys, apoptosis or detachment of podocytes lead to denuded areas of glomerular basement membrane, which adhere to the Bowman's capsule. This then results in misdirected filtration of urine into the paraglomerular and paratubular space, finally leading to nephron loss.[10–12] This 'podocyte depletion' theory is supported by findings that podocytes are found in the urine from patients and experimental animals with proteinuria.[22–28]

In NPHS1 kidneys, podocytes undoubtedly play a major role both in the protein leakage and in triggering the sclerotic process. Our previous electron microscopic analysis[7] and the results in this work, however, suggest that it may not be question of simple 'podocyte depletion', but rather a more complex interplay of podocytes with mesangial and endothelial cells. Similar phenomena have been observed in rats with anti-Thy 1.1 glomerulonephritis when treated with puromycin aminonucleoside injections as well as in transgenic mice where podocyte damage has been caused by a podocyte-specific immunotoxin.[29,30] Podocytes in NPHS1 kidneys undergo phenotypic changes, such as foot process effacement, which is typical for nephrotic diseases. They also show hypertrophy, which was evident both in electron and light microscopy and further supported by the findings that upregulation of cell cycle promoters cyclin A and D1, and downregulation of cell cycle kinase inhibitor p57 (together a sign of hypertrophic and hyperplastic phenotype) were found in parallel with low rate of proliferation in podocytes.[31] Importantly, the podocytes in NPHS1 kidneys did not proliferate, as is the case in the collapsing variant of FSGS.[32]

Shedding of podocytes into urine is believed to reflect the podocyte injury, and has been reported in several types of human kidney diseases.[24–28] Analysis of urine from NPHS1 patients revealed that the number of podocalyxin-positive cells in NPHS1 patients (median 15.9 cells/ml) was quite close to that previously found in patients with FSGS (4.2 and 1.3 cells/ml)[25,26] and lupus nephritis (6.2 cells/ml).[27] So, it seems clear that podocytes detach from the glomerular basement membrane in NPHS1 kidneys. Whether this reflects some primary event or is a consequence of the glomerular tuft damage remains to be solved.

We were especially interested in possible synechiae of the glomerular (denuded) capillaries with the Bowman's capsule leading to misdirected filtration of capillary blood or urine. Attachment of the glomerular tuft with the Bowman's capsule was frequently seen in NPHS1 and control kidneys in direct microscopy and this finding was difficult to interpret. However, if misdirected filtration and filtrate spreading were an important early event leading to glomerular sclerosis and nephron degeneration, segmental lesions should have been seen in a substantial proportion of the hundreds of well-preserved (functional) NPHS1 glomeruli analyzed. This was clearly not the case. We found no local protrusions of the glomerular tuft into the paratubular spaces or paraglomerular space, as reported in FSGS.[10–12]

In conclusion, the results suggest that in NPHS1 kidneys the role of mesangial sclerosis and stenosis of glomerular capillaries are pivotal for the destruction of the glomerulus, and possibly the downfall of the entire nephron. Which

mediators are important in the interplay of damaged podocytes with mesangial and endothelial cells remains to be solved.

MATERIALS AND METHODS

Tissue and urine samples

A total of 49 children with NPHS1 (age 4–44 months) were nephrectomized at the Hospital for Children and Adolescents, University of Helsinki, Finland, between the years 1986 and 2003. Twenty-nine of the patients were homozygotes for Fin-major mutation, nine had Fin-major/Fin-minor genotype and four were Fin-minor homozygotes.[5,6] In addition, one patient had Fin-major/C465Y, one had Fin-major/IVS26-1 g→a, and one Fin-major/C465Y genotype. No knowledge of the mutations in four samples was available. All patients had a severe nephrotic syndrome from the birth and were treated with daily albumin infusions to supplement the continuous heavy protein losses.

Routine formalin-fixed paraffin-embedded samples were prepared from the kidneys and the rest of the renal cortex was snap-frozen in liquid nitrogen and stored at −70°C. The glomeruli for scanning electron microscopy were isolated under dissection microscope and processed as described previously.[7] As controls, we used eight normal adult kidneys (age 47–58 years) removed for transplantation. These kidneys proved unsuitable for transplantation mainly because of vascular abnormalities. Formalin-fixed paraffin-embedded sections and snap-frozen samples were collected. The cadaver kidneys had to be used as controls, as fresh tissue samples from normal infant kidneys were not possible to obtain.

Fresh urine samples were obtained from four NPHS1 children aged 3–10 months, five pediatric patients with normal kidney function, and five healthy adults. Fifteen samples were collected from NPHS1 children and 12 samples from the control group. The urine specimens were processed within 2 h after voiding.[33]

The study protocol was approved by the ethical committee of the Hospital for Children and Adolescents of the University of Helsinki and conformed to the principles outlined in the Declaration of Helsinki.

Antibodies

The following antibodies were purchased from Dako (Glostrup, Denmark): B-cell lymphoma-2 (M0887), CD20cy (M0755), CD34 (M7165), CD68 (M0876), MIB-1 (M7240), p53 (M7001), and vimentin (M7020). Antibodies against cyclin A (NCL-Cyclin A), cyclin D1 (NCL-cyclin D1-GM), and WT1 (NCL-WT-1-6FH2) were bought from Novocastra (Newcastle upon Tyne, UK). From Abcam (Cambridge, Cambridgeshire, UK) were antibodies against CD3 (ab828) and CD14 (ab8679). Antibodies against CD13 (MS-1079) and p57 (MS-1062-P) were bought from Neomarkers (Fremont, CA, USA). In addition, we used mast cell tryptase (Mob 347) (Diagnostic BioSystems, Pleasanton, CA, USA), podocalyxin (AF1658) (R&D Systems, Minneapolis, MN, USA), and ZO-1 (61-7300) (Zymed Laboratories, San Francisco, CA, USA) antibodies. All these primary antibodies were unconjugated, and dilutions from 1:10 to 1:250 were used.

We used the following markers for different inflammatory cell types: CD13 for monocytes, CD68 for macrophages, CD14 for monocytes and macrophages and some of their subpopulations, mast cell tryptase for activated mast cells, CD3 for T-lymphocytes, and CD20cy for B-lymphocytes.

Light microscopy

The histological lesions in the NPHS1 glomeruli were evaluated by light microscopy from paraffin-embedded tissue sections stained with hematoxylin and eosin or periodic acid silver methenamin (PASM). Glomerular sclerosis was correlated to the age at nephrectomy in 49 NPHS1 kidneys as described previously (Figure 1c).[19]

The progression of glomerular damage was analyzed by grading 10 features of glomerular histology in 1528 glomeruli of 20 NPHS1 kidneys (age range 4–44 months, median age 8 months). The parameters were: the increase of mesangial matrix and cell content, the size of the urinary space, the thickness of the Bowman's basement membrane, the size of the mesangial hilus, hypertrophy and the number of PEC, and the amount of periglomerular fibrosis and periglomerular inflammation. In addition, the presence of crescents, tipping of the glomerular tuft into the tubular pole, peritubular changes, and a possible hyperplasia of the podocyte layer were noted on each glomerulus.

Immunohistochemistry

For the immunofluorescence stainings, the cryosections (5 μm) of the kidney samples were fixed with 3.5% paraformaldehyde or acetone, depending on the antibody used. The stainings were performed in a traditional way. Sections used as negative controls were incubated in phosphate-buffered saline instead of a primary antibody. Podocalyxin and ZO-1-positive cells and granular material in the urine sediments of NPHS1 patients and controls were studied by immunofluorescence as described previously.[28]

Immunoperoxidase stainings were performed on the sections of formalin-fixed, paraffin-embedded renal samples in a conventional way. To improve antibody penetration, microwave treatment in 10 mM citric acid or Dako Target Retrieval Solution (Dako) were used. Amplification of the primary antibody reaction was achieved by incubating the sections with biotinylated secondary antibody (Vector Laboratories Inc., Burlingame, CA, USA). Immunoperoxidase staining of cryosections, fixed with 3.5% paraformaldehyde or acetone, was performed similarly.

The image analysis program NIH ImageJ 1.32j (National Institutes of Health, Bethesda, MD, USA) was used to calculate the area fraction of a particular immunostained component. The area fraction of capillary lumens was calculated using the same program with a manual selection of the calculated area. The proportion of black-to-white pixels in the image was calculated as a percentage.[34] All immunohistochemical data were analyzed from at least five control and six NPHS1 kidneys.

TUNEL

The occurrence of apoptosis in glomerular cells was analyzed by monitoring the presence of DNA fragmentation.[35] Slides were analyzed by light microscopy after counterstaining with hematoxylin. Cells exhibiting dark brown staining from the colorimetric reaction were considered positive for DNA fragmentation. Nine NPHS1 kidneys with a histology ranging from nearly normal to severely damaged were analyzed together with five control kidneys. As positive controls, we used testis samples with abundant apoptosis.

Statistics

Data are presented as mean ± s.d. Two-tailed P-values < 0.05 (Student's t-test) were considered significant.

REFERENCES

1. Eddy AA. Progression in chronic kidney disease. *Adv Chronic Kidney Dis* 2005; **12**: 353–365.
2. Boute N, Gribouval O, Roselli S *et al.* NPHS2, encoding the glomerular protein podocin, is mutated in autosomal recessive steroid-resistant nephrotic syndrome. *Nat Genet* 2000; **24**: 349–354.
3. Kaplan JM, Kim SH, North KN *et al.* Mutations in ACTN4, encoding alpha-actinin-4, cause familial focal segmental glomerulosclerosis. *Nat Genet* 2000; **24**: 251–256.
4. Habib R, Loirat C, Gubler MC *et al.* The nephropathy associated with male pseudohermaphroditism and Wilms' tumor (Drash syndrome): a distinctive glomerular lesion, report of 10 cases. *Clin Nephrol* 1985; **24**: 269–278.
5. Kestila M, Lenkkeri U, Mannikko M *et al.* Positionally cloned gene for a novel glomerular protein – nephrin – is mutated in congenital nephrotic syndrome. *Mol Cell* 1998; **1**: 575–582.
6. Patrakka J, Kestila M, Wartiovaara J *et al.* Congenital nephrotic syndrome (NPHS1): features resulting from different mutations in Finnish patients. *Kidney Int* 2000; **58**: 972–980.
7. Lahdenkari AT, Lounatmaa K, Patrakka J *et al.* Podocytes are firmly attached to glomerular basement membrane in kidneys with heavy proteinuria. *J Am Soc Nephrol* 2004; **15**: 2611–2818.
8. Fogo AB. Animal models of FSGS: lessons for pathogenesis and treatment. *Semin Nephrol* 2003; **23**: 161–171.
9. D'Agati V. Pathologic classification of focal segmental glomerulosclerosis. *Semin Nephrol* 2003; **23**: 117–134.
10. Gassler N, Elger M, Kranzlin B *et al.* Podocyte injury underlies the progression of focal segmental glomerulosclerosis in the fa/fa Zucker rat. *Kidney Int* 2001; **60**: 106–116.
11. Kriz W, Gretz N, Lemley KV. Progression of glomerular diseases: is the podocyte the culprit? *Kidney Int* 1998; **54**: 687–697.
12. Kriz W, LeHir M. Pathways to nephron loss starting from glomerular diseases – insights from animal models. *Kidney Int* 2005; **67**: 404–419.
13. Huttunen NP, Rapola J, Vilska J, Hallman N. Renal pathology in congenital nephrotic syndrome of Finnish type: a quantitative light microscopic study on 50 patients. *Int J Pediatr Nephrol* 1980; **1**: 10–16.
14. Vats AN, Costello B, Mauer M. Glomerular structural factors in progression of congenital nephrotic syndrome. *Pediatr Nephrol* 2003; **18**: 234–240.
15. Nikolic-Paterson DJ, Lan HY, Hill PA, Atkins RC. Macrophages in renal injury. *Kidney Int Suppl* 1994; **45**: S79–S82.
16. Hooke DH, Gee DC, Atkins RC. Leukocyte analysis using monoclonal antibodies in human glomerulonephritis. *Kidney Int* 1987; **31**: 964–972.
17. Le Hir M, Besse-Eschmann V. A novel mechanism of nephron loss in a murine model of crescentic glomerulonephritis. *Kidney Int* 2003; **63**: 591–599.
18. Thomas DB, Franceschini N, Hogan SL *et al.* Clinical and pathologic characteristics of focal segmental glomerulosclerosis pathologic variants. *Kidney Int* 2006; **69**: 920–926.
19. Kuusniemi AM, Lapatto R, Holmberg C *et al.* Kidneys with heavy proteinuria show fibrosis, inflammation, and oxidative stress, but no tubular phenotypic change. *Kidney Int* 2005; **68**: 121–132.
20. Fine LG, Orphanides C, Norman JT. Progressive renal disease: the chronic hypoxia hypothesis. *Kidney Int Suppl* 1998; **65**: S74–78.
21. Kang DH, Kanellis J, Hugo C *et al.* Role of the microvascular endothelium in progressive renal disease. *J Am Soc Nephrol* 2002; **13**: 806–816.
22. Petermann AT, Pippin J, Krofft R *et al.* Viable podocytes detach in experimental diabetic nephropathy: potential mechanism underlying glomerulosclerosis. *Nephron Exp Nephrol* 2004; **98**: e114–e123.
23. Petermann AT, Krofft R, Blonski M *et al.* Podocytes that detach in experimental membranous nephropathy are viable. *Kidney Int* 2003; **64**: 1222–1231.
24. Vogelmann SU, Nelson WJ, Myers BD, Lemley KV. Urinary excretion of viable podocytes in health and renal disease. *Am J Physiol Renal Physiol* 2003; **285**: F40–F48.
25. Nakamura T, Ushiyama C, Suzuki S *et al.* The urinary podocyte as a marker for the differential diagnosis of idiopathic focal glomerulosclerosis and minimal-change nephrotic syndrome. *Am J Nephrol* 2000; **20**: 175–179.
26. Hara M, Yanagihara T, Kihara I. Urinary podocytes in primary focal segmental glomerulosclerosis. *Nephron* 2001; **89**: 342–347.
27. Nakamura T, Ushiyama C, Suzuki S *et al.* Urinary podocytes for the assessment of disease activity in lupus nephritis. *Am J Med Sci* 2000; **320**: 112–116.
28. Hara M, Yamamoto T, Yanagihara T *et al.* Urinary excretion of podocalyxin indicates glomerular epithelial cell injuries in glomerulonephritis. *Nephron* 1995; **69**: 397–403.
29. Morioka Y, Koike H, Ikezumi Y *et al.* Podocyte injuries exacerbate mesangial proliferative glomerulonephritis. *Kidney Int* 2001; **60**: 2192–2204.
30. Matsusaka T, Xin J, Niwa S *et al.* Genetic engineering of glomerular sclerosis in the mouse via control of onset and severity of podocyte-specific injury. *J Am Soc Nephrol* 2005; **16**: 1013–1023.
31. Marshall CB, Shankland SJ. Cell cycle and glomerular disease: a minireview. *Nephron Exp Nephrol* 2006; **102**: e39–e48.
32. Detwiler RK, Falk RJ, Hogan SL, Jennette JC. Collapsing glomerulopathy: a clinically and pathologically distinct variant of focal segmental glomerulosclerosis. *Kidney Int* 1994; **45**: 1416–1424.
33. Segasothy M, Lau TM, Birch DF *et al.* Immunocytologic dissection of the urine sediment using monoclonal antibodies. *Am J Clin Pathol* 1998; **90**: 691–696.
34. Furness PN. The use of digital images in pathology. *J Pathol* 1997; **183**: 253–263.
35. Tilly JL. Use of the terminal transferase DNA labelling reaction for the biochemical and in situ analysis of apoptosis. In: Celis JE (ed). *Cell Biology: A Laboratory Handbook*. vol. 1 Academic Press: San Diego, 1994 pp 330–337.